Coordinated Optimal Network Reconfiguration and Voltage Regulator/DER Control for Unbalanced Distribution Systems

Yikui Liu, Student Member, IEEE, Jie Li, Member, IEEE, Lei Wu, Senior Member, IEEE,

Abstract—Network reconfiguration has long been used by distribution system operators to achieve certain operation objectives such as reducing system losses or regulating bus voltages. In emerging distribution systems with a proliferation of distributed energy resources (DERs), co-optimizing network topology and DERs' dispatches could further enhance such operational benefits. This paper focuses on the optimal network reconfiguration problem of distribution systems via an unbalanced AC optimal power flow (ACOPF) framework, which rigorously addresses operation characters of unbalanced network, DERs, and voltage regulators (VRs). Two VR models with continuous and discrete tap ratios are studied and compared. The proposed co-optimization problem is formulated as a mixed-integer chordal relaxation based semidefinite programming (MISDP) model with binary variables indicating line-switching statuses and tap positions. Several acceleration strategies by studying the structure of distribution networks are explored for reducing the number of binary variables and enhancing the computational performance. Case studies on modified IEEE 34-bus and 392-bus systems illustrate the effectiveness of the proposed approach.

Index Terms—DER, distribution system operator, network reconfiguration, unbalanced distribution system, voltage regulator.

	Nomenclature						
Indices:							
d, g	Index of loads/ DERs						
l(n,m)	Index of a lines and ideal transformer with two terminal buses n and m						
m, n	Indices of buses						
S	Index of static var compensators (SVCs) and static synchronous compensators						
1 -	(STATCOMs)						
ϕ, ho	Indices of phases						
Sets:							
$D, \mathcal{G}, \mathcal{R}, B, \mathcal{S}$	Set of constant power loads/conventional DERs/ renewable DERs/ buses/ SVCs and STATCOMs						
$oldsymbol{e}^{\phi}$	Standard basis vector of $\mathbb{R}^{3\times 1}$, i.e., $[1\ 0\ 0]^T/$						
	$[0\ 1\ 0]^T/[0\ 0\ 1]^T$ for phase $a/b/c$						
\mathcal{L},\mathcal{T}	Set of lines/ideal transformers						
$oldsymbol{ au}_l$	Set of tap ratios for ideal transformer <i>l</i>						
\mathbb{R},\mathbb{C}	Set of real/complex numbers						
Ψ	Set of phases, i.e., $\Psi = \{a, b, c\}$						

This work was supported in part by the U.S. National Science Foundation grants PFI:BIC-1534035 and CNS-1647135. Y. Liu, J. Li, and L. Wu are with Electrical and Computer Engineering Department, Clarkson University, Potsdam, NY 13699 USA. (E-mail: yikliu, jieli, lwu @clarkson.edu).

Switching action flag

Variables:

 b_l

Active/reactive power injection at phase ϕ of
the distribution substation bus (indexed as 0)
Active/reactive power through VR connected
at phase ϕ of bus n
Active/reactive power injection from DER g
Reactive power injection of SVC and
DSTATCOM s
Tap ratio of ideal transformer l
Line/ideal transformer status indicator, 1 for
ON and 0 for OFF
Auxiliary status indicators for line/ideal
transformer l that connects buses m and n
Complex voltage of phase ϕ at bus n
Vector of complex voltages, i.e., $V =$
$[V_0^a \ V_0^b \ V_0^c \ V_{N+R}^a \ V_{N+R}^b \ V_{N+R}^c]^T$
Voltage vector of bus n , i.e., = $[V_n^a V_n^b V_n^c]^T$
Total number of buses/VRs

В Allowed number of switching actions P_d, Q_d Active/reactive power demand of fixed load d Forecasted active power generation of renewable DER g PFPower factor U_l Line/ideal transformer initial status indicator Given voltage values of the distribution $\hat{\boldsymbol{V}}_0$ substation bus, i.e., $\hat{\mathbf{V}}_0 = [\hat{V}_0^a \ \hat{V}_0^b \ \hat{V}_0^c]^T$ Matrix/vector with all zeros $(\cdot)^{min}, (\cdot)^{max}$ Lower/upper bound of a certain parameter

(·) min , (·) max Lower/upper bound of a certain parameter (·) $^{\phi,\rho}$ Element corresponding to phase ϕ and phase ρ in a matrix

Symbols:

 $card(\cdot)$ Cardinality of set $re(\cdot)$ Real part of a complex number $tr(\cdot), |\cdot|$ Trace/ magnitude $(\cdot)^T, (\cdot)^*, (\cdot)^H$ Transpose/ conjugate/ transpose and conjugate

I. INTRODUCTION

Distribution systems are usually operated under a radial configuration for two reasons: protection devices can be effectively coordinated with simple parameter settings, and magnitudes of ground-fault currents are limited. However, distribution systems are exclusively designed as loops or meshed networks, for guaranteeing reliability and flexibility in fault isolation and load restoration. Indeed, by taking advantage of the meshed network design, DSOs adopt network reconfiguration strategies for optimizing system operations and achieving certain objectives such as system loss reduction and voltage regulation. Network reconfiguration can be

conducted by adjusting statuses of sectionalizers/tie switches which are normally closed/open to reshape the network topology.

Distribution system network reconfiguration is inherently a mixed-integer nonlinear programming (MINLP) problem, which includes binary variables for indicating open/closed statuses of configurable lines, as well as AC power flow equations representing nonlinear/nonconvex relationships between voltages and power injections of individual buses. Thus, solving the distribution system network reconfiguration problem is challenging in terms of computational burden and solution quantity. Heuristic algorithms, such as branch exchange method [1]-[3], genetic algorithm [4]-[5], and particle swarm optimization [6], were commonly used to solve the problem. However, solution consistency cannot be guaranteed and solution quality is hard to justify. Specifically, different initial values such as first breaking loop and first generation of genes in genetic algorithm could highly impact final solutions. Moreover, without any information about the best possible optimal solution, it is difficult to quantitatively evaluate optimality of a solution from heuristic algorithms, which could be far from the global optimum.

Convex relaxation technique was first introduced by X. Bai et al. in [7] to solve AC optimal power flow (ACOPF) problem, which was formulates as a semidefinite programming (SDP) model aiming at obtaining global optimal solutions with a high computational efficiency. Reference [8] extended the application to unbalanced distribution systems. A well-cited pioneering paper [9] builds up the theoretical basis for applying convex relaxation technique in the ACOPF problem. Recently, convex relaxation techniques have been applied for solving nonconvex reconfiguration problems in an attempt to obtain global optimal solutions. Reference [10] modeled the network reconfiguration problem of balanced distribution systems as a mixed-integer second-order cone programming (MISOCP) model, in which topology constraints were used to preserve network radiality and connectivity. Several convex models are compared in [11], including mixed-integer quadratic, mixed-integer quadratically constrained, and MISOCP models, for solving balanced distribution system reconfiguration problems. Moreover, [12] proposed a branch exchange based algorithm to solve the reconfiguration problem of balanced distribution systems, in which the inner optimal power flow problem is formulated as a SOCP model.

However, references [10]-[12] exclusively focused on balanced distribution systems, whereas the actual distribution systems are inherently unbalanced with unbalanced three-phase loads, untransposed line segments, and single- or two-phase laterals, especially for medium and low voltage systems [13]. In unbalanced distribution systems, couplings between three-phase currents cannot be offset, while neglecting such couplings will undoubtedly cause significant inaccuracy and may not provide physically viable operation instructions to DSOs. Therefore, unbalanced distribution system network reconfiguration models and solution approaches are eagerly needed, as indicated in recent works [14]-[17]. References

[14]-[16] solved unbalanced reconfiguration problems via heuristic algorithms, while solution consistency and quality continue to be major concerns. The study in [17] convexified the unbalanced reconfiguration problem by including a line current sparsity penalty term into the line loss minimization objective, while the distributed energy resources (DER) dispatches were considered as constants. However, the coefficient of the penalty term needs to be carefully tuned for simultaneously ensuring network radiality and solution optimality.

Furthermore, in emerging distribution systems with the proliferation of DERs, the value of network reconfiguration has been clearly illustrated [18], while coordinating dispatches of DERs with network reconfiguration presents new challenges for the optimal operation. Specifically, as voltage magnitudes are sensitive to active power injections of DERs due to high resistance to reactance ratios of distribution lines [19], a deeper penetration of DERs is likely to cause voltage issues. In recognizing that, voltage regulators (VRs), static var compensators (SVCs), distribution static synchronous compensators (DSTATCOMs), and shunt capacitor banks are widely used in distribution systems to maintain voltage levels at load buses, and their operation statuses should also be cooptimized to derive better network reconfiguration solutions. Reference [20] considered the voltage regulation effect of substation transformer with continuous tap ratio and modeled a balanced single-phase distribution reconfiguration problem as a mixed-integer nonlinear programming (MINLP) model, which is solved by generalized benders decomposition. However, voltage regulators with discrete tap ratios have not been considered under any three-phase unbalanced distribution system reconfiguration study.

This paper studies the optimal network reconfiguration problem of unbalanced distribution systems with DERs and voltage regulation devices. The objective is to minimize the total system operation cost. Two typical categories of DERs are considered, with conventional DERs directly connected to distribution network and renewable DERs connected via electronic inverters. Optimal operations of voltage regulation devices, including VRs, SVCs, DSTATCOMs, and shunt capacitor banks, are modeled. The entire problem is formulated as a mixed-integer SDP (MISDP) model based on chordal relaxation technique [21]-[22]. The MISDP model is solved via a branch-and-bound based algorithm, in which a series of binary variable relaxation subproblems are computed sequentially. Each binary variable relaxation subproblem is an SDP problem that can be solved via primal-dual interior point algorism, in which binary variables are either fixed as 1/0 if they have been branched, or relaxed as continuous in [0,1] if they are to be determined. Moreover, as illustrated in literature that chordal relaxation technique can improve computational performance of SDP based OPF problems as compared to conventional rank relaxation technique [23], it could also help reduce calculation time of MISDP based three-phase distribution system reconfiguration problem studied in this paper. Moreover, the MISDP solution process requires no initial values and solution quality can be effectively evaluated

via lower bound provided by branch-and-bound algorism. Moreover, if a solution satisfies certain conditions as discussed in this paper, corresponding optimal power flow results (i.e., dispatches of DERs, voltages, and real/reactive power flows) are global optimal with respect to the obtained configuration solution.

Major contributions of this paper are:

- 1) The three-phase unbalanced distribution system reconfiguration problem, which co-optimizes distribution network topology and operation of various DERs and voltage regulation devices, is formulated as a chordal relaxation based MISDP model for the first time. The proposed model also optimally coordinates inverters of renewable DERs, VRs, capacitor banks, and SVCs within the three-phase distribution system reconfiguration framework to effectively regulate voltage levels within their limits while achieving the minimum total operation cost of distribution systems.
- 2) Several acceleration strategies are proposed by studying distribution network structures and VR models with continuous and discrete tap ratios. These strategies would reduce the number of binary variables associated with line switching statuses as well as auxiliary continuous variables, and in turn enhance computational performance.

The rest of the paper is organized as follows. The unbalanced distribution system reconfiguration problem is described in Section II. The chordal relaxation based MISDP formulation and two VR models are introduced in Section III. Numerical case studies are conducted in Section IV, and the conclusions are drawn in Section V.

II. UNBALANCED DISTRIBUTION SYSTEM RECONFIGURATION

Unbalanced distribution systems with wye connected threeconductor solidly grounded or four-conductor solidly multigrounded neutral are studied. In such systems, impedance matrix of line l can be simulated as a 3×3 phase frame complex matrix Y_1 . For single- and two- phase lines, elements in Y_l corresponding to missing phases are zeroes. Similarly, line shunt matrices can be represented as a 3×3 phase frame complex matrix Y_1^s .

A. System Component Modeling

- Constant Loads: A constant power load (CPL) d is modeled via fixed active and reactive power demands P_d and Q_d . A constant impedance load (CIL) d is simulated by a 3×3 matrix Y_n^d shunted at bus n. For single- and two- phase CILs, missing-phase elements in Y_n^d are zeros.
- DERs: Conventional DERs $(g \in G)$ and renewable DERs $(g \in \mathcal{R})$ are modeled as (1) and (2) respectively. Operation cost of a conventional DER is represented via (1a). In current distribution systems, instead of directly owning renewable DERs, it is a common practice that utilities purchase electricity from renewable DER owners through power purchase agreements (PPA) [24] at long-term fixed prices. Thus, the energy feed-in tariff of a renewable DER is represented as (2a), where η_g represents the inverter power

loss factor. Renewable DERs, like photovoltaics and wind turbines, are usually connected to an AC distribution network via electronic inverters [25]. (1b) and (1c) represent power output limits of conventional DERs. (2b) indicates that renewable DERs can be dispatched between 0 and the forecast value. Inverter capacity limit $P_g^2 + Q_g^2 \le \left(S_g^{max}\right)^2$ is presented in the Schur complement form as in (2c). (1d) and (2d) are power factor constraints.

$$\begin{aligned} &C_g\big(P_g\big) = c_{g2} \cdot \big(P_g\big)^2 + c_{g1} \cdot P_g + c_{g0}; & g \in \boldsymbol{\mathcal{G}} & \text{(1a)} \\ &P_g^{min} \leq P_g \leq P_g^{max}; & g \in \boldsymbol{\mathcal{G}} & \text{(1b)} \\ &Q_g^{min} \leq Q_g \leq Q_g^{max}; & g \in \boldsymbol{\mathcal{G}} & \text{(1c)} \end{aligned}$$

$$Q_q^{min} \le Q_q \le Q_q^{max}; \qquad g \in \mathbf{G}$$
 (1c)

$$Q_{g} \leq Q_{g} \leq Q_{g} , \qquad g \in \mathbf{G}$$

$$\frac{PF_{g}^{min}}{\sqrt{1 - (PF_{g}^{min})^{2}}} Q_{g} \leq P_{g} \leq \frac{PF_{g}^{max}}{\sqrt{1 - (PF_{g}^{max})^{2}}} Q_{g}; \qquad g \in \mathbf{G}$$

$$C_{g}(P_{g}) = c_{g1} \cdot [(1 + \eta_{g}) \cdot P_{g}]; \qquad g \in \mathbf{R}$$

$$0 \leq P \leq P^{est} \cdot \qquad g \in \mathbf{R}$$

$$0 \leq P \leq P^{est} \cdot \qquad g \in \mathbf{R}$$

$$(2a)$$

$$C_g(P_g) = c_{g1} \cdot [(1 + \eta_g) \cdot P_g];$$
 $g \in \mathcal{R}$ (2a)

$$0 \le P_g \le P_g^{est}; \qquad g \in \mathcal{R} \qquad (2b)$$

$$\begin{bmatrix} \left(S_{g}^{max}\right)^{2} & P_{g} & Q_{g} \\ P_{g} & 1 & 0 \\ Q_{g} & 0 & 1 \end{bmatrix} \geqslant 0; \qquad g \in \mathcal{R} \quad (2c)$$

$$\frac{P_{g}^{min}}{\sqrt{1 - \left(P_{g}^{min}\right)^{2}}} Q_{g} \leq P_{g} \leq \frac{P_{g}^{max}}{\sqrt{1 - \left(P_{g}^{max}\right)^{2}}} Q_{g}; \qquad g \in \mathcal{R} \quad (2d)$$

$$\frac{\frac{PF_g^{min}}{\int_{1-\left(PF_g^{min}\right)^2}^2}Q_g \le P_g \le \frac{PF_g^{max}}{\int_{1-\left(PF_g^{max}\right)^2}^2}Q_g; \qquad g \in \mathcal{R} \qquad \text{(2d)}$$

• Voltage Regulation Devices: Different types of reactive power compensition devices are considered. A static capacitor bank c provides specific capacitance Y_n^c shunted at bus n, which can be combined with CILs at that bus to derive impedance matrix of bus n as $Y_n = Y_n^d + Y_n^c$. An SVC/DSTATCOM s can inject or withdraw reactive power at the connecting bus without involving active power as in (3).

$$Q_s^{min} \le Q_s \le Q_s^{max}; \qquad s \in \mathbf{S} \quad (3)$$

A three-phase wye-wye solidly grounded VR is modeled as an impedance in series with an ideal transformer l, as shown in Fig. 1 [26]. m represents the virtual bus connected to the secondary side of ideal transformer l. Three-phase tap ratios are equal to each other, i.e., the taps are ganged. The ideal transformer is modeled as in (4), where P_n^{ϕ} , P_m^{ϕ} and Q_n^{ϕ} , Q_m^{ϕ} are active and reactive powers transmitted through transformer l. Two-phase and single-phase VRs can be simliarly modeled. $r_l \cdot V_n^{\phi} = V_m^{\phi};$

$$r_{l} \cdot v_{n'} = v_{m'};$$

$$P_{n}^{\phi} = P_{m}^{\phi}; \quad Q_{n}^{\phi} = Q_{m}^{\phi}; \qquad r_{l} \in \boldsymbol{\tau}_{l}, l(n, m) \in \boldsymbol{\mathcal{T}}$$

$$r_{l} \in \boldsymbol{\tau}_{l}, l(n, m) \in \boldsymbol{\mathcal{T}}$$

Fig. 1 Equivalent circuit of a voltage regulation transformer

B. Distribution Network Modeling

paper consideres distribution system network reconfiguration by switching ON/OFF sectionalizers and tie switches equipped on three-phase lines for dynamically adjusting the network topology. For single- and two- phase lines, sectionalizers are primarily used for protection purposes to isolate faults, and tie switches for reconfiguration is rarely reported in literature or engineering practices [14]-[17].

To study the distribution system network reconfiguration problem, the concept of maximum meshed sub-network is first

 $\textstyle \sum_{m \in \{m \mid l(n,m) \in \left(\mathcal{L} - \mathcal{L}_{3}^{o}\right)\}} tr \left(\boldsymbol{\bar{\Phi}}_{P,l}^{\phi} \cdot [\boldsymbol{V}_{n}^{T} \ \boldsymbol{V}_{m}^{T}]^{T} \cdot [\boldsymbol{V}_{n}^{H} \ \boldsymbol{V}_{m}^{H}]\right) + \sum_{m \in \{m \mid l(n,m) \in \mathcal{L}_{3}^{o}\}} \left[tr \left(\boldsymbol{\bar{\Phi}}_{P,l}^{\phi} \cdot [\boldsymbol{V}_{n}^{T} \ \boldsymbol{V}_{m}^{T}]^{T} \cdot [\boldsymbol{V}_{n}^{H} \ \boldsymbol{V}_{m}^{H}]\right) \cdot \boldsymbol{u}_{l}\right] + tr \left(\boldsymbol{\Phi}_{P,n}^{\phi} \cdot \boldsymbol{V}_{n} \cdot \boldsymbol{V}_{m}^{T}\right) + tr \left(\boldsymbol{\bar{\Phi}}_{P,n}^{\phi} \cdot \boldsymbol{V}_{n}^{T}\right) + tr \left(\boldsymbol{\bar{\Phi}}_{P,$ V_n^H) = $\sum_{a \in G_n^{\phi} \cup \mathcal{R}_n^{\phi}} P_g - \sum_{d \in \mathcal{D}_n^{\phi}} P_d + \Lambda_n \cdot P_n^{\phi}$ $\sum_{m \in \{m \mid l(n,m) \in (\mathcal{L} - \mathcal{L}_3^o)\}} tr(\bar{\boldsymbol{\Phi}}_{Q,l}^{\phi} \cdot [\boldsymbol{V}_n^T \ \boldsymbol{V}_m^T]^T \cdot [\boldsymbol{V}_n^H \ \boldsymbol{V}_m^H]) + \sum_{m \in \{m \mid l(n,m) \in \mathcal{L}_3^o\}} \left[tr(\bar{\boldsymbol{\Phi}}_{Q,l}^{\phi} \cdot [\boldsymbol{V}_n^T \ \boldsymbol{V}_m^T]^T \cdot [\boldsymbol{V}_n^H \ \boldsymbol{V}_m^H]) \cdot u_l \right] + tr(\boldsymbol{\Phi}_{Q,n}^{\phi} \cdot \boldsymbol{V}_n \cdot \boldsymbol{V}_n \cdot \boldsymbol{V}_n) \cdot u_l \cdot$

defined. A maximum meshed sub-network refers to the maximum sub-network in which any pair of nodes is

$$\sum_{m \in \{m \mid l(n,m) \in (\mathcal{L} - \mathcal{L}_{3}^{o})\}} tr(\bar{\boldsymbol{\Phi}}_{Q,l}^{\phi} \cdot [\boldsymbol{V}_{n}^{T} \ \boldsymbol{V}_{m}^{T}]^{T} \cdot [\boldsymbol{V}_{n}^{H} \ \boldsymbol{V}_{m}^{H}]) + \sum_{m \in \{m \mid l(n,m) \in \mathcal{L}_{3}^{o}\}} [tr(\bar{\boldsymbol{\Phi}}_{Q,l}^{\phi} \cdot [\boldsymbol{V}_{n}^{T} \ \boldsymbol{V}_{m}^{T}]^{T} \cdot [\boldsymbol{V}_{n}^{H} \ \boldsymbol{V}_{m}^{H}]) \cdot u_{l}] + tr(\boldsymbol{\Phi}_{Q,n}^{\phi} \cdot \boldsymbol{V}_{n} \ \boldsymbol{V}_{n}^{H}) = \sum_{g \in \boldsymbol{\mathcal{G}}_{n}^{\phi} \cup \boldsymbol{\mathcal{R}}_{n}^{\phi}} Q_{g} - \sum_{d \in \boldsymbol{\mathcal{D}}_{n}^{\phi}} Q_{d} + \sum_{s \in \boldsymbol{\mathcal{S}}_{n}^{\phi}} Q_{s} + \Lambda_{n} \cdot Q_{n}^{\phi}$$

$$(7)$$

connected via at least two paths. Considering a distribution network with all sectionalizers and tie switches being initially ON, lines that are not contained in any maximum meshed subnetwork must be ON to ensure network connectivity. In turn, only status indicators of lines that are contained in maximum meshed sub-networks and equipped with sectionalizers/tie switches need to be defined as binary decision variables.

 \mathcal{L}_{3}^{w} is defined as the set of three-phase lines equipped with sectionalizers/tie switches contained in maximum meshed subnetworks. When all sectionalizers/tie switches are closed, a distribution system would contain several maximum meshed sub-networks. \mathcal{L}_3^o and \mathcal{T}_3^o are sets of three-phase lines and ideal transformers contained in maximum meshed subnetworks, and \mathcal{H} is the set of starting points assigned for each maximum meshed sub-networks. Topology constraints (5) guarantee the network radiality and connectivity [10]. (5a) describes the upstream-downstream topological relationship between nodes n and m that are directly connected by a line or an ideal transformer in maximum meshed sub-networks. $v_l^n =$ 0 means n is the adjacent upstream node, and otherwise downstream node. (5b) forces that a starting point is the upstream node of all its adjacent nodes. (5c) indicates that except for starting points, each node can only have one upstream node. (5d) restricts that ideal transformers and threephase lines without switches will be kept ON.

Constraint (6) restricts the number of switching actions which affects the life span of sectionalizers/tie switches.

$$\begin{aligned} v_l^n + v_l^m &= u_l; \quad v_l^n, v_l^m, u_l \in \{0,1\}; \quad l(n,m) \in \mathcal{L}_3^o \cup \mathcal{T}_3^o \quad \text{(5a)} \\ v_l^n &= 0; \qquad \qquad n \in \mathcal{H}, \quad l(n,m) \in (\mathcal{L}_3^o \cup \mathcal{T}_3^o) \quad \text{(5b)} \\ \sum_{l(n,m) \in (\mathcal{L}_3^o \cup \mathcal{T}_3^o)} v_l^n &= 1; \qquad n \notin \mathcal{H} \quad \qquad \text{(5c)} \\ u_l &= 1; \qquad \qquad l(n,m) \in \mathcal{T}_3^o \cup (\mathcal{L}_3^o - \mathcal{L}_3^w) \quad \text{(5d)} \\ \sum_{l(n,m) \in (\mathcal{L}_3^o \cup \mathcal{T}_3^o)} b_l \leq B \quad \qquad \text{(6a)} \end{aligned}$$

$$b_l \ge u_l - U_l; \quad b_l \ge U_l - u_l; \quad l(n, m) \in (\mathcal{L}_3^o \cup \mathcal{T}_3^o)$$
 (6b)

C. Three-phase Power Flow Modeling

In an unbalanced distribution system, total complex power withdrawn at phase ϕ of bus n includes three parts: power withdrawn via adjacent lines not contained in maximum meshed sub- networks, power withdrawn via adjacent lines contained in maximum meshed sub-networks, and power withdrawn via CILs and shunt capacity banks. Summation of the three parts is equal to net complex power injections from DERs, CPLs, and ideal transforms at phase ϕ of bus n. Such nodal active and reactive power balances are represented in matrix trace forms (7). In formulation (7a) for example, the first two terms of left side are active power injections from lines not contained and contained in maximum meshed subnetworks, matrix $\left\{ \sum_{m \in \{m \mid l(n,m) \in (\mathcal{L} - \mathcal{L}_3^0)\}} V_n^{\phi} \cdot \left[\sum_{\rho \in \Psi} (Y_l^{\phi,\rho} + Y_l^{s,\phi,\rho}) \cdot V_n^{\rho} - Y_l^{\phi,\rho} \right] \right\}$

 $V_m^
hoig]^*ig\} \qquad ext{and} \qquad re\left\{\sum_{m\in\{m\mid l(n,m)\in\mathcal{L}_3^o\}}u_l\cdot V_n^\phi\cdotig[\sum_{
ho\inoldsymbol{\Psi}}ig(Y_l^{\phi,
ho}+ig)^\phi
ight\}$ $(Y_l^{s,\phi,\rho}) \cdot V_n^{\rho} - (Y_l^{\phi,\rho} \cdot V_m^{\rho})^*$. The third term is active power injection from CILs and shunt capacity banks, i.e., the matrix form of $re\left\{V_n^{\phi}\cdot\left(\sum_{\rho\in\Psi}\boldsymbol{Y}_n^{\phi,\rho}\cdot V_n^{\rho}\right)^*\right\}$. While the three terms in the left side of (7b) are the imaginary parts of the three above formulations. Λ_n , $\overline{\Phi}_{P,l}^{\phi}$, $\overline{\Phi}_{Q,l}^{\phi}$, $\Phi_{P,n}^{\phi}$, and $\Phi_{Q,n}^{\phi}$ are defined as:

$$\Lambda_n = \begin{cases}
-1 & \text{if } \exists l(n,m) \in \mathcal{T} \\
1 & \text{if } \exists l(m,n) \in \mathcal{T} \text{ or } n = 0 \\
0 & \text{otherwise}
\end{cases} \tag{8a}$$

$$\mathbf{Y}_{l}^{\phi} = \begin{bmatrix} \left(\mathbf{e}^{\phi}\right)^{T} & \mathbf{0}_{1\times3} \end{bmatrix}^{T} \cdot \begin{bmatrix} \left(\mathbf{e}^{\phi}\right)^{T} & \mathbf{0}_{1\times3} \end{bmatrix} \cdot \begin{bmatrix} \mathbf{Y}_{l} + \mathbf{Y}_{l}^{s} & -\mathbf{Y}_{l} \\ -\mathbf{Y}_{l} & \mathbf{Y}_{l} + \mathbf{Y}_{l}^{s} \end{bmatrix}$$
(8b)

$$\bar{\boldsymbol{\Phi}}_{P,l}^{\phi} = \frac{1}{2} \cdot \left(\mathbf{Y}_{l}^{\phi} + \left(\mathbf{Y}_{l}^{\phi} \right)^{H} \right); \qquad \bar{\boldsymbol{\Phi}}_{Q,l}^{\phi} = \frac{j}{2} \cdot \left(\mathbf{Y}_{l}^{\phi} - \left(\mathbf{Y}_{l}^{\phi} \right)^{H} \right)^{T}$$
(8c)

$$\boldsymbol{Y}_{n}^{\phi} = \left(\boldsymbol{e}^{\phi}\right)^{T} \cdot \boldsymbol{e}^{\phi} \cdot \boldsymbol{Y}_{n} \tag{8d}$$

$$\mathbf{\Phi}_{P,n}^{\phi} = \frac{1}{2} \cdot \left(\mathbf{Y}_{n}^{\phi} + \left(\mathbf{Y}_{n}^{\phi} \right)^{H} \right); \quad \mathbf{\Phi}_{Q,n}^{\phi} = \frac{j}{2} \cdot \left(\mathbf{Y}_{n}^{\phi} - \left(\mathbf{Y}_{n}^{\phi} \right)^{H} \right) \quad (8e)$$
 $\mathbf{D}_{n}^{\phi}, \mathbf{G}_{n}^{\phi}, \mathbf{R}_{n}^{\phi}, \text{ and } \mathbf{S}_{n}^{\phi} \text{ are sets of CPLs, conventional and renewable DERs, and SVCs/DSTATCOMs connected at phase ϕ of bus n .$

D. Distribution System Network Reconfiguration Problem

Given electricity price c_0 of all three phases at the distribution substation bus, the network reconfiguration problem is formulated as (9). The objective (9a) is to minimize the total distribution system operation cost, in which the first term represents total production cost of conventional and renewable DERs and the second term represents purchasing cost of importing electricity from the main grid through the substation bus. (9c) is bus voltage magnitude limit, where $\left(V_n^{\phi}\right)^* \cdot V_n^{\phi}$ for each phase ϕ is represented via a compact matrix form $tr(\boldsymbol{\Phi}_{V,n}^{\phi}\cdot\boldsymbol{V}_n\cdot\boldsymbol{V}_n^H)$ with $\boldsymbol{\Phi}_{V,n}^{\phi}=\boldsymbol{e}^{\phi}\cdot\left(\boldsymbol{e}^{\phi}\right)^T$. Current limit of three-phase lines is modeled as (9d) to prevent line thermal limit violations, where current I_l^{ϕ} of line l at phase ϕ can be calculated as $\sum_{\rho \in \Psi} Y_l^{\phi, \rho} \cdot \left(V_n^{\rho} - V_m^{\rho} \right)$ and in turn squared line current magnitude $|I_i^{\phi}|^2$ is represented via a compact matrix form $tr(\bar{\boldsymbol{\Phi}}_{l,l}^{\phi} \cdot [\boldsymbol{V}_n^T \ \boldsymbol{V}_m^T]^T \cdot [\boldsymbol{V}_n^H \ \boldsymbol{V}_m^H])$, with $\overline{\boldsymbol{\Phi}}_{l,l}^{\phi} = [\boldsymbol{Y}_{l} \quad -\boldsymbol{Y}_{l}]^{H} \cdot \boldsymbol{e}^{\phi} \cdot (\boldsymbol{e}^{\phi})^{T} \cdot [\boldsymbol{Y}_{l} \quad -\boldsymbol{Y}_{l}].$ (9e) sets voltages of the distribution substation bus. Variable sets C = $\{P_a, Q_a, Q_s\}$ and $I = \{v_l^n, u_l\}$.

$$\min_{\boldsymbol{V}_{n},\boldsymbol{c},\boldsymbol{I},r_{l}} \left\{ \sum_{g \in \boldsymbol{\mathcal{G}} \cup \boldsymbol{\mathcal{R}}} C_{g}(P_{g}) + \sum_{\phi \in \boldsymbol{\Psi}} c_{0} \cdot P_{0}^{\phi} \right\}$$
 (9a)
Subject to: constraints (1)-(7) (9b)

$$\left(\left| V_{n}^{\phi} \right|^{min} \right)^{2} \leq tr \left(\boldsymbol{\Phi}_{V,n}^{\phi} \cdot \boldsymbol{V}_{n} \cdot \boldsymbol{V}_{n}^{H} \right) \leq \left(\left| V_{n}^{\phi} \right|^{max} \right)^{2}$$

$$tr \left(\overline{\boldsymbol{\Phi}}_{l,l}^{\phi} \cdot [\boldsymbol{V}_{n}^{T} \ \boldsymbol{V}_{m}^{T}]^{T} \cdot [\boldsymbol{V}_{n}^{H} \ \boldsymbol{V}_{m}^{H}] \right) \cdot u_{l} \leq \left(\left| I_{l}^{\phi} \right|^{max} \right)^{2}$$

$$l(n,m) \in \boldsymbol{\mathcal{L}}_{3}^{o} \text{ (9d)}$$

$$\begin{split} & [V_{0}^{a}, V_{0}^{b}, V_{0}^{c}]^{T} = \widehat{\boldsymbol{V}}_{0} & (9e) \\ & \sum_{m \in \{m \mid l(n,m) \in (\mathcal{L}-\mathcal{L}_{3}^{o})\}} tr\left(\boldsymbol{\bar{\Phi}}_{P,l}^{\phi} \cdot \begin{bmatrix} \boldsymbol{W}_{n,n} & \boldsymbol{W}_{n,m} \\ \boldsymbol{W}_{m,n} & \boldsymbol{W}_{m,m} \end{bmatrix}\right) + \sum_{m \in \{m \mid l(n,m) \in \mathcal{L}_{3}^{o}\}} tr\left(\boldsymbol{\bar{\Phi}}_{P,l}^{\phi} \cdot \begin{bmatrix} \boldsymbol{W}_{n,l} & \boldsymbol{W}_{n,m} \\ \boldsymbol{W}_{m,n} & \boldsymbol{W}_{m,l} \end{bmatrix}\right) + tr\left(\boldsymbol{\Phi}_{P,n}^{\phi} \cdot \boldsymbol{W}_{n,n}\right) = \\ & \sum_{g \in \mathcal{G}_{n}^{\phi} \cup \mathcal{R}_{n}^{\phi}} P_{g} - \sum_{d \in \mathcal{D}_{n}^{\phi}} P_{d} + \Lambda_{n} \cdot P_{n}^{\phi} \\ & \sum_{m \in \{m \mid l(n,m) \in (\mathcal{L}-\mathcal{L}_{3}^{o})\}} tr\left(\boldsymbol{\bar{\Phi}}_{Q,l}^{\phi} \cdot \begin{bmatrix} \boldsymbol{W}_{n,n} & \boldsymbol{W}_{n,m} \\ \boldsymbol{W}_{m,n} & \boldsymbol{W}_{m,m} \end{bmatrix}\right) + \sum_{m \in \{m \mid l(n,m) \in \mathcal{L}_{3}^{o}\}} tr\left(\boldsymbol{\bar{\Phi}}_{Q,l}^{\phi} \cdot \begin{bmatrix} \boldsymbol{W}_{n,n} & \boldsymbol{W}_{n,m} \\ \boldsymbol{W}_{m,n} & \boldsymbol{W}_{m,l} \end{bmatrix}\right) + tr\left(\boldsymbol{\Phi}_{Q,n}^{\phi} \cdot \boldsymbol{W}_{n,n}\right) = \\ & \sum_{g \in \mathcal{G}_{n}^{\phi} \cup \mathcal{R}_{n}^{\phi}} Q_{g} - \sum_{d \in \mathcal{D}_{n}^{\phi}} Q_{d} + \sum_{s \in \mathcal{S}_{n}^{\phi}} Q_{s} + \Lambda_{n} \cdot Q_{n}^{\phi} \end{split} \tag{11f}$$

III. CHORDAL RELAXATION FOR UNBALANCED DISTRIBUTION SYSTEM NETWORK RECONFIGURATION

A. Chordal Relaxation Based Reformulation

The proposed distribution system network reconfiguration problem (9) includes three types of nonlinear and nonconvex terms $V_n^{\phi} \cdot \left(V_m^{\rho}\right)^* \cdot u_l$, $V_n^{\phi} \cdot \left(V_m^{\rho}\right)^*$, and $r_l \cdot V_n^{\phi}$. Indeed, based on author's previous work [23], the first two types of nonlinear terms can be directly relaxed as semidefinite constraints which are convex. Thus, if the third term could be properly convexified, (9) can be reformulated as a MISDP model after chordal relaxation. A new variable $W_{n,m}^{\phi,\rho}$ is thus introduce to substitute the nonlinear term $V_n^{\phi} \cdot \left(V_m^{\rho}\right)^*$ in (9). However, implementing such a variable substitution will introduce a bi-linear term $W_{n,m}^{\phi,\rho}\cdot u_l$, a product of a continuous variable and a binary variable. By further defining an auxiliary variable $\mathcal{W}_{n.m.l}^{\phi,\rho} = W_{n,m}^{\phi,\rho} \cdot u_l$, the bi-linear term can be equivalently linearized as:

$$-M \cdot u_{l} \leq \mathcal{W}_{n,m,l}^{\phi,\rho} \leq M \cdot u_{l}; \qquad l(n,m) \in \mathcal{L}_{3}^{o} \qquad (10a)$$

$$-M \cdot (1-u_{l}) \leq W_{n,m}^{\phi,\rho} - \mathcal{W}_{n,m,l}^{\phi,\rho} \leq M \cdot (1-u_{l});$$

$$l(n,m) \in \mathcal{L}_{3}^{o} \qquad (10b)$$

where *M* is a complex constant $\left[(1+j) \cdot |V_n^{\phi}|^{max} \cdot |V_m^{\rho}|^{max} \right]$ In (10), "\ge " ("\le ") means both real and imaginary parts are no smaller (no larger) than corresponding right-hand-side values. After this, the distribution system network reconfiguration problem (9) can be reformulated as (11) applying chordal relaxation, where $V_n \cdot V_n^H$ and $V_n \cdot V_m^H$ are substituted by matrices $W_{n,n}$ and $W_{n,m}$. The objective function (11a) corresponds to (9b). The first term is represented in an epigraph form with auxiliary constraints (11c) and (11d), where (11c) is in Schur complement form. (11e)-(11f) represent the active and reactive power balance constraints for each phase at each bus equivalent to (7a)-(7b) in (9). (11g) corresponds to (4), representing the voltage relationship between primary and secondary sides of an ideal transformer. (11h)-(11i) are voltage and current limits equivalent to (9c)-(9d). Distribution substation bus voltages (9e) are expressed in the matrix form (11j). (11k) represents positive semidefinite constraints corresponding to lines not contained in maximum meshed sub-network which could be derived according to the author's previous work in [23]. (111) represents positive semidefinite constraints corresponding to switchable lines contained in maximum meshed sub-networks. $\boldsymbol{W}_{n,m}$ and $\boldsymbol{\mathcal{W}}_{n,l}$ are defined in (12). Specifically, when $u_l = 1$ (line l is

switched ON), $W_{n,n}^{\phi,\rho}$ will be equal to $W_{n,n,l}^{\phi,\rho}$ according to (10b), and in turn $W_{n,n}$ will be equal to $W_{n,l}$. Thus, (111) works equivalently to (11k). When $u_l = 0$ (line l is switched OFF, that is the line is physically not existed in the circuit), the power injection from line l is zero. According to (10a), when $u_l=0$, $\mathcal{W}_{n,n,l}^{\phi,
ho}$ and $\mathcal{W}_{m,m,l}^{\phi,
ho}$ are all zeros and in turn $m{\mathcal{W}}_{n,l}$ and $\mathcal{W}_{m,l}$ are **0** in (111). Furthermore, positive semidefinite constraints (111) force $W_{n,m}$ and $W_{m,n}$ to be 0 since the diagonal elements of matrix $\begin{bmatrix} \boldsymbol{w}_{n,l} & \boldsymbol{W}_{n,m} \\ \boldsymbol{w}_{m,n} & \boldsymbol{w}_{m,l} \end{bmatrix}$ are all zeros and thus the entire matrix $\begin{bmatrix} \boldsymbol{w}_{n,l} & \boldsymbol{W}_{n,m} \\ \boldsymbol{w}_{m,n} & \boldsymbol{w}_{m,l} \end{bmatrix} = \mathbf{0}$, which effectively removes the power injection components from switched OFF line l in power balance constraints (11e)-(11f).

$$min_{w_{n,m}} w_{n,l} \alpha_g, c, I, r_l \left\{ \sum_{g \in \mathcal{G} \cup \mathcal{R}} \alpha_g + \sum_{\phi \in \Psi} c_0 \cdot P_0^{\phi} \right\}$$
 (11a)

$$\begin{bmatrix} \alpha_{g} - c_{g1} \cdot P_{g} - c_{g0} & -\sqrt{c_{g2}} \cdot P_{g} \\ -\sqrt{c_{g2}} \cdot P_{g} & 1 \end{bmatrix} \geqslant 0; \qquad g \in \mathbf{G} \quad (11c)$$

$$\alpha_{g} - c_{g1} \cdot (1 + \eta_{g}) \cdot P_{g} = 0; \qquad g \in \mathbf{R} \quad (11d)$$

$$\mathbf{W}_{m,m} = r_{l}^{2} \cdot \mathbf{W}_{n,n}; \qquad r_{l} \in \mathbf{r}_{l}, \ l(n,m) \in \mathbf{T} \quad (11g)$$

$$\alpha_{a} - c_{a1} \cdot (1 + \eta_{a}) \cdot P_{a} = 0;$$
 $g \in \mathcal{R}$ (11d)

$$\boldsymbol{W}_{m,m} = r_l^2 \cdot \boldsymbol{W}_{n,n}; \qquad r_l \in \boldsymbol{r}_l, \ l(n,m) \in \boldsymbol{T}$$
 (11g)

$$\left(\left|V_{n}^{\phi}\right|^{min}\right)^{2} \le tr\left(\boldsymbol{\Phi}_{V,n}^{\phi} \cdot \boldsymbol{W}_{n,n}\right) \le \left(\left|V_{n}^{\phi}\right|^{max}\right)^{2} \tag{11h}$$

$$tr\left(\overline{\boldsymbol{\Phi}}_{l,l}^{\phi} \cdot \begin{bmatrix} \boldsymbol{W}_{n,l} & \boldsymbol{W}_{n,m} \\ \boldsymbol{W}_{m,n} & \boldsymbol{W}_{m,l} \end{bmatrix}\right) \leq \left(\left|I_{l}^{\phi}\right|^{\max}\right)^{2}; \quad l(n,m) \in \mathcal{L}_{3}^{o} \quad (11i)$$

$$\begin{bmatrix} W_{0,0}^{a,a} & W_{0,0}^{a,b} & W_{0,0}^{a,c} \\ W_{0,0}^{b,a} & W_{0,0}^{b,b} & W_{0,0}^{b,c} \\ W_{0,0}^{c,a} & W_{0,0}^{c,b} & W_{0,0}^{c,c} \end{bmatrix} = \widehat{\boldsymbol{V}}_0 \cdot (\widehat{\boldsymbol{V}}_0)^H$$
(11j)

$$\begin{bmatrix} \mathbf{W}_{0,0} & \mathbf{W}_{0,0} & \mathbf{W}_{0,0} \end{bmatrix} \\ \begin{bmatrix} \mathbf{W}_{n,n} & \mathbf{W}_{n,m} \\ \mathbf{W}_{m,n} & \mathbf{W}_{m,m} \end{bmatrix} \geqslant 0; \qquad l(n,m) \in \mathcal{L} - \mathcal{L}_3^o \qquad (11k) \\ \begin{bmatrix} \mathbf{W}_{n,l} & \mathbf{W}_{n,m} \\ \mathbf{W}_{m,n} & \mathbf{W}_{m,l} \end{bmatrix} \geqslant 0; \qquad l(n,m) \in \mathcal{L}_3^o \qquad (11l)$$

$$\begin{bmatrix} \mathbf{\mathcal{W}}_{n,l} & \mathbf{\mathcal{W}}_{n,m} \\ \mathbf{\mathcal{W}}_{m,n} & \mathbf{\mathcal{W}}_{m,l} \end{bmatrix} \geqslant 0; \qquad l(n,m) \in \mathcal{L}_3^o$$
 (111)

$$\boldsymbol{W}_{n,m} = \begin{bmatrix} W_{n,m}^{a,a} W_{n,m}^{a,b} W_{n,m}^{a,c} \\ W_{n,m}^{b,a} W_{n,m}^{b,b} W_{n,m}^{b,c} \\ W_{n,m}^{c,a} W_{n,m}^{c,b} W_{n,m}^{c,c} \end{bmatrix}; \boldsymbol{W}_{n,l} = \begin{bmatrix} W_{n,n,l}^{a,a} W_{n,n,l}^{a,b} W_{n,n,l}^{a,c} \\ W_{n,n,l}^{b,a} W_{n,n,l}^{b,b} W_{n,n,l}^{b,c} \\ W_{n,n,l}^{c,a} W_{n,n,l}^{c,b} W_{n,n,l}^{c,c} \end{bmatrix}$$
(12)

It can be seen that if (11g) is excluded, problem (11) becomes a MISDP model. In the following section, we study how to reformulate (11g) to make (11) an MISDP model.

B. Reformulation of Voltage Regulators

In this paper, two ideal transformer models are studied. The first one regards the tap ratio as a continues variable within the range of $[r_l^{min}, r_l^{max}]$. Thus, (11g) could be reformulated as a positive semidefinite relaxation form (13) according to [23].

$$(r_l^{max})^2 \cdot \boldsymbol{W}_{n,n} - \boldsymbol{W}_{m,m} \geq 0; \ \boldsymbol{W}_{m,m} - (r_l^{min})^2 \cdot \boldsymbol{W}_{n,n} \geq 0;$$

$$r_l^{min} \leq r_l \leq r_l^{max};$$

$$l(n,m) \in \boldsymbol{\mathcal{T}}$$
 (13)

The second model formulates the tap ratio as a discrete variable in (14). That is, the tap ratio of an ideal transformer can only take certain discrete values $(r_l^{min} + c_l \cdot k)$ for $0 \le$ $k \le 2K_l$, i.e., 0 to $2K_l$ taps with the tap ratio step of $c_l =$ $(r_l^{max} - r_l^{min})/2K_l$. Binary variable $R_{k,l}$ represents the tap position indicator. (14b) forces that tap positions are

$$\boldsymbol{W}_{m,m} = \left[\sum_{k=0}^{2K_l} (r_l^{min} + c_l \cdot k)^2 \cdot R_{k,l}\right] \cdot \boldsymbol{W}_{n,n}; \quad l(n,m) \in \boldsymbol{\mathcal{T}}$$
(14a)

$$\sum_{k=0}^{2R_l} R_{k,l} = 1; R_{k,l} \in \{0,1\}$$

 $\sum_{k=0}^{2K_{l}} R_{k,l} = 1; \qquad R_{k,l} \in \{0,1\} \qquad (14b)$ Nonlinear terms $R_{k,l} \cdot W_{n,n}^{\phi,\rho}$ in (14a) can be further linearized as (15), where $W_{n,l,k}^{\phi,\rho}$ is an auxiliary variable to substitute $R_{k,l} \cdot W_{n,n}^{\phi,\rho}$. Thus, (11g) can be reformulated as (15) and (14b). For each three-phase ideal transformer $l(n, m) \in \mathcal{T}$, $2K_1 + 1$ binary and $6 \times (2K_1 + 1)$ continuous variables will be introduced in this discrete linearization model, which may cause significant computational burden as compared to the continuous linearization model (13).

$$-M \cdot R_{k,l} \le \mathcal{W}_{n,l,k}^{\phi,\rho} \le M \cdot R_{k,l} \tag{15a}$$

$$W_{n,n}^{\phi,\rho} - (1 - R_{k,l}) \cdot M \le W_{n,l,k}^{\phi,\rho}$$

$$\leq W_{n,n}^{\phi,\rho} + \left(1 - R_{k,l}\right) \cdot M \tag{15b}$$

$$-M \cdot R_{k,l} \leq \mathcal{W}_{n,l,k}^{\phi,\rho} \leq M \cdot R_{k,l}$$

$$W_{n,n}^{\phi,\rho} - (1 - R_{k,l}) \cdot M \leq \mathcal{W}_{n,l,k}^{\phi,\rho}$$

$$\leq W_{n,n}^{\phi,\rho} + (1 - R_{k,l}) \cdot M$$

$$W_{m,m}^{\phi,\rho} = \sum_{k=0}^{2K_{l}} \left[\left(r_{l}^{min} + c_{l} \cdot k \right)^{2} \cdot \mathcal{W}_{n,l,k}^{\phi,\rho} \right]$$
(15a)
$$(15b)$$

C. MISDP Model for the Network Reconfiguration Problem

Depending on whether VRs are formulated via continuous or discrete tap ratios, the proposed unbalanced distribution system network reconfiguration problem could be formulated as an MISDP model, either in the form of (16) or (17).

• Reconfiguration model with continuous tap ratios (Rec-c): $min_{W_{n,m},W_{n,l},\alpha_g,c,l,r_l} \{ \sum_{g \in \mathcal{G} \cup \mathcal{R}} \alpha_g + \sum_{\phi \in \mathcal{\Psi}} c_0 \cdot P_0^{\phi} \}$ (16a)

• Reconfiguration model with discrete tap ratios (Rec-d):

$$\min_{\boldsymbol{W}_{n,m},\boldsymbol{W}_{n,l},\alpha_{g},\boldsymbol{c},\boldsymbol{I},r_{l},\boldsymbol{W}_{n,n,k}^{\phi,\rho},R_{k,l}} \left\{ \sum_{g \in \boldsymbol{\mathcal{G}} \cup \boldsymbol{\mathcal{R}}} \alpha_{g} + \sum_{\phi \in \boldsymbol{\Psi}} c_{0} \cdot P_{0}^{\phi} \right\}$$

$$(17a)$$

After solving Rec-c or Rec-d, matrices $W_{n,m}$ and $W_{m,n}$ corresponding to lines with $u_1 = 0$ are all zeros. If matrices

 $[\boldsymbol{W}_{n,n} \ \boldsymbol{W}_{n,m}]$ corresponding to lines with $u_l = 1$ and lines $[\boldsymbol{W}_{m,n} \, \boldsymbol{W}_{m,m}]$

not contained in maximum meshed sub-network are all rank one, and in the same time, (18) is satisfied, the optimal solution to the original problem (9) can be recovered [23].

$$(\hat{r}_l)^2 \cdot \boldsymbol{W}_{n,n} = \boldsymbol{W}_{m,m}; \qquad \qquad l(n,m) \in \boldsymbol{\mathcal{T}}$$
 (18)

 \hat{r}_l represents the optimal tap ratio solution from Rec-c or Rec-d. Otherwise, if rank one condition and (18) are not satisfied simultaneously, the solution of (16) or (17) is an infeasible solution to the original problem (9), which indicates the relaxed convex models (16) or (17) is not tight enough. However, based on our extensive experience in different distribution system studies, such an infeasible situation rarely

happens and finding a practical system that cannot be exactly solved may not be easy according to our study.

IV. CASE STUDIES

In this section, an illustrative example is first presented to explain the maximum meshed sub-network concept and the representation of power flow equations in (9) and (11). After that, two distribution systems are studied to illustrate the effectiveness and computational performance of the proposed unbalanced distribution network reconfiguration solution.

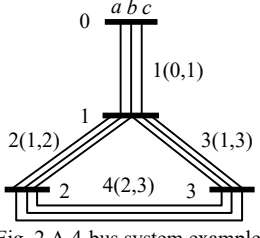
A. A Small Illustration Example

A 4-bus system example shown in Fig. 2 is first used to illustrate the maximum meshed sub-network concept and the representation of power flow equations in (9) and (11).

All four lines in the system are three-phase lines. It is observed that buses 0 and 1 are connected through only one path, while each pair of buses 1, 2 and 3 is connected via two paths. That is, line 1(0,1) must be ON to keep connectivity, while only two of the other three lines 2(1,2), 3(1,3), 4(2,3)have to be ON for ensuring connectivity. Thus, according to the definition of maximum meshed sub-network, 1-2-3 constitutes a maximum meshed sub-network.

For this 4-bus system, active power flow equations of phase a at bus 1 are written as in (19) corresponding to (7a). Specifically, in (19), the first three terms are respectively active power flows through lines 1(0,1), 2(1,2), and 3(1,3), and the fourth term is active power flow through line shunt admittance and constant impedance load. u_2 and u_3 in (19) are binary variables indicating ON/OFF statuses of lines 2(1,2) and 3(1,3). For instance, when u_2 is 0, $tr(\bar{\Phi}_{P,2}^a \cdot [V_1^T \ V_2^T]^T \cdot$ $[\boldsymbol{V}_1^H \ \boldsymbol{V}_2^H] \cdot u_2$ and $tr(\overline{\boldsymbol{\Phi}}_{0,2}^a \cdot [\boldsymbol{V}_1^T \ \boldsymbol{V}_2^T]^T \cdot [\boldsymbol{V}_1^H \ \boldsymbol{V}_2^H]) \cdot u_2$ are 0, which indicate line 2(1,2) is switched OFF and power flow carrying is disabled. Status indicator of line 1(0,1) is not needed because it must be ON as discussed above.

Variable substitutions to reformulate (19) are defined in (20). After variable substitution with auxiliary variables, (19) can be equivalently represented as in (21). Similarly, when u_2 is zero, based on (10a), all elements in $\boldsymbol{\mathcal{W}}_{1,2}$ and $\boldsymbol{\mathcal{W}}_{2,2}$ are zeros and in turn $\begin{bmatrix} \mathbf{W}_{1,2} & \mathbf{W}_{1,2} \\ \mathbf{W}_{2,1} & \mathbf{W}_{2,2} \end{bmatrix}$ is forced to be a zero matrix because of semidefinite constraint (111) and zero diagonal elements. It shows that line 2(1,2) is switched OFF and power flow carrying is disabled. In addition, line 1(0,1) must be ON to keep connectivity, thus $\boldsymbol{\mathcal{W}}_{0,1}$ and $\boldsymbol{\mathcal{W}}_{1,1}$ do not need to be defined.



$$tr\big(\boldsymbol{\bar{\Phi}}_{P.1}^a\cdot[\boldsymbol{V}_0^T\ \boldsymbol{V}_1^T]^T\cdot[\boldsymbol{V}_0^H\ \boldsymbol{V}_1^H]\big)+tr\big(\boldsymbol{\bar{\Phi}}_{P.2}^a\cdot[\boldsymbol{V}_1^T\ \boldsymbol{V}_2^T]^T\cdot$$

$$\begin{split} & [\boldsymbol{V}_{1}^{H} \ \boldsymbol{V}_{2}^{H}] \big) \cdot \boldsymbol{u}_{2} + tr \big(\overline{\boldsymbol{\Phi}}_{P,3}^{a} \cdot [\boldsymbol{V}_{1}^{T} \ \boldsymbol{V}_{3}^{T}]^{T} \cdot [\boldsymbol{V}_{1}^{H} \ \boldsymbol{V}_{3}^{H}] \big) \cdot \boldsymbol{u}_{3} + \\ & tr \big(\overline{\boldsymbol{\Phi}}_{P,1}^{a} \cdot \boldsymbol{V}_{1} \cdot \boldsymbol{V}_{1}^{H} \big) = -\sum_{d \in \mathcal{D}_{1}^{a}} P_{d} \\ & [\boldsymbol{V}_{0}] \cdot \begin{bmatrix} \boldsymbol{V}_{0} \\ \boldsymbol{V}_{1} \end{bmatrix}^{H} \rightarrow \begin{bmatrix} \boldsymbol{W}_{0,0} \ \boldsymbol{W}_{0,1} \\ \boldsymbol{W}_{1,0} \ \boldsymbol{W}_{1,1} \end{bmatrix}; \begin{bmatrix} \boldsymbol{V}_{1} \\ \boldsymbol{V}_{2} \end{bmatrix} \cdot \begin{bmatrix} \boldsymbol{V}_{1} \\ \boldsymbol{V}_{2} \end{bmatrix}^{H} \rightarrow \begin{bmatrix} \boldsymbol{W}_{1,1} \ \boldsymbol{W}_{1,2} \\ \boldsymbol{W}_{2,1} \ \boldsymbol{W}_{2,2} \end{bmatrix} \\ \begin{bmatrix} \boldsymbol{V}_{1} \\ \boldsymbol{V}_{3} \end{bmatrix} \cdot \begin{bmatrix} \boldsymbol{V}_{1} \\ \boldsymbol{V}_{3} \end{bmatrix}^{H} \rightarrow \begin{bmatrix} \boldsymbol{W}_{1,1} \ \boldsymbol{W}_{1,3} \\ \boldsymbol{W}_{3,1} \ \boldsymbol{W}_{3,3} \end{bmatrix}; \\ tr \left(\overline{\boldsymbol{\Phi}}_{P,1}^{a} \cdot \begin{bmatrix} \boldsymbol{W}_{0,0} \ \boldsymbol{W}_{0,1} \\ \boldsymbol{W}_{1,0} \ \boldsymbol{W}_{1,1} \end{bmatrix} \right) + tr \left(\overline{\boldsymbol{\Phi}}_{P,2}^{a} \cdot \begin{bmatrix} \boldsymbol{W}_{1,2} \ \boldsymbol{W}_{1,2} \\ \boldsymbol{W}_{2,1} \ \boldsymbol{W}_{2,2} \end{bmatrix} \right) + \\ tr \left(\overline{\boldsymbol{\Phi}}_{P,3}^{a} \cdot \begin{bmatrix} \boldsymbol{W}_{1,3} \ \boldsymbol{W}_{1,3} \\ \boldsymbol{W}_{3,1} \ \boldsymbol{W}_{3,3} \end{bmatrix} \right) + tr \left(\boldsymbol{\Phi}_{P,1}^{a} \cdot \boldsymbol{W}_{1,1} \right) = -\sum_{d \in \mathcal{D}_{1}^{a}} P_{d} \end{aligned} \tag{21}$$

B. The Modified IEEE 34-bus System Case Study

The modified IEEE 34-bus system shown in Fig. 3 includes 34 original buses and 2 virtual buses 7 and 20 for the two VRs. Four tie-lines 8-32, 13-28, 17-31, and 30-33 equipped with tie switches are added, shown as dashed lines with three slashes in Fig. 2. The modified distribution system includes only one maximum meshed sub-network as highlighted via dashed lines in Fig. 2. All 20 three-phase lines in the maximum meshed sub-network are considered switchable. Lower and upper bounds of tap ratios of the two VRs are 0.95 and 1.05. For the discrete tap ratio setting, K_l is set as 4, and c_l as 0.0125. A single-phase SVC, SVCA, is connected at phase a of bus 12, with reactive power limits of [-550kVar, 850kVar]. A three-phase conventional DER, GA, is connected as bus 17. A three-phase renewable DER as bus 30, GB, has an inverter loss factor 0.02. Power factor limits of both DERs are set as [0, 1]. Configuration data of GA and GB are shown in Tables I-II. Electricity price at the distribution substation bus is 10¢/kWh. Voltages at the distribution substation bus are $1.05 \angle 0^{\circ}$ p.u., $1.05 \angle -120^{\circ}$ p.u., and $1.05 \angle 120^{\circ}$ p.u.. For all other buses, lower and upper bounds of phase voltage magnitudes are 0.95p.u. and 1.05p.u.. Current limits of all three-phase lines are set as 0.352kA. The initial statues of entities in $\mathcal{L}_3^0 \cup$ \mathcal{T}_3^o are considered as ON $(U_1=1)$ and in turn B is set as $card(\mathcal{L}_3^o \cup \mathcal{T}_3^o)$ minus R+N-1. Other detailed configuration data can be found in [27].

The formulated MISDP problems are solved by integrating the branch-and-bound (BAB) solver in Yalmip [28] to handle binary variables and Mosek [29] to solve SDP problems at individual BAB nodes. Threshold of relative gap in the BAB algorithm is set as 0.01%. As the rank of a matrix is equal to the number of its nonzero eigenvalues, 1×10^{-4} is set as threshold to determine if a numerical eigenvalue is nonzero.

The following three cases are studied.

- Case 1: Network reconfiguration with CPLs only.
- Case 2: Network reconfiguration with DERs and SVCs.
- Case 3: Network reconfiguration with both DERs and CILs.

TABLE I DATA OF THE CONVENTIONAL DER GA

Phase	c_{g2} (×10 ⁻⁵ ¢/kWh ²)	<i>c</i> _{<i>g</i>1} (¢/kWh)	c_{g0} (c)	Pg ^{max} (kW)	0	Q_g^{max} (kvar)	Q_g^{min} (kvar)
а	189	6.1	0	1680	200	720	100
b	203	6.3	0	1680	200	780	100
c	195	6.0	0	1680	200	700	100

TABLE II DATA OF THE RENEWABLE DER GB

Phase	$c_{g1} (\rm \rlap/kWh)$	P_g^{max} (kW)	P_g^{min} (kW)	S_g^{max} (kVA)
а	5.1	1250	0	1400
b	5.2	1250	0	1350
С	5.6	1250	0	1350

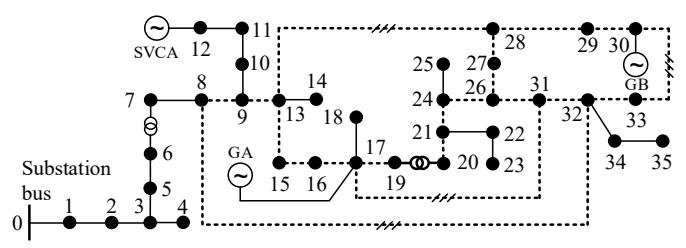


Fig. 3 The modified IEEE 34-bus distribution system

Case 1: This case studies distribution system network reconfiguration with CPLs only. Without DERs, objective function of the original problem is degenerated to minimizing electricity purchase cost from the substation $\sum_{\phi \in \Psi} c_0 \cdot P_0^{\phi}$. Indeed, as P_0^{ϕ} covers all demands and distribution losses, this case is equivalent to minimizing distribution losses.

Both Rec-c and Rec-d models are tested. Rec-c is completed in 31 seconds. All variable matrices $\begin{bmatrix} \mathbf{W}_{n,n} & \mathbf{W}_{n,m} \\ \mathbf{W}_{m,n} & \mathbf{W}_{m,m} \end{bmatrix}$ corresponding to switched-on lines (i.e., $u_l = 1$) and lines not contained in maximum meshed sub-networks are rank one, and (18) is satisfied. That is, a feasible and good-enough solution to (9) could be recovered from solution to Rec-c. In addition, voltages of phase c at virtual buses 7 and 20, which are secondary sides of two ideal transformers, reach their upper bounds. The reason is that, a higher voltage would mitigate distribution losses by reducing line currents, and in turn minimize the total operation cost. Rec-d is solved in 90 seconds, while all variable matrices corresponding to switched-on lines are also rank one. However, extra variables introduced in (14b)-(15) show noticeable impact on computational efficiency when considering discrete tap ratios.

Detailed solutions to Rec-c and Rec-d are compared in Table III. It shows that the network topology configuration results of both models are identical. Indeed, the system after network reconfiguration contains two main radial laterals (i.e., buses 14-23 and buses 8, 24-26, 29-35) with 10 and 11 buses respectively, while total loads of the two laterals are very close (i.e., 5670kW and 6270kW). On the other hand, operation cost of Rec-d is slightly higher than that of Rec-c, because optimal tap ratio solutions in Rec-d can only take discrete values. In fact, since voltages of buses 7 and 20 both reach their upper bounds in Rec-c, optimal tap ratios of Rec-d are equal to the largest discrete tap values that are smaller than those in Rec-c. For further comparison, two base cases with continuous VR tap ratios (BS-c) and discrete VR tap ratios (BS-d) while neglecting network reconfiguration are also studied. As shown in Table III, both BS-c and BS-d present much higher operation costs associated with larger distribution system losses. Significant loss reductions, namely 49.08% and 49.07%, can be achieved in Rec-c and Rec-d, respectively.

		(\$)	(kW)	(6-7)	(19-20)
Rec-c	21-24,26-27,28-29,17-31	96.35	963.5	1.0377	1.0144
Rec-d	21-24,26-27,28-29,17-31	96.40	964.0	1.0375	1.0125
BS-c	17-31, 8-32, 13-28, 30-33	189.20	1892.0	1.0372	1.0384
BS-d	17-31, 8-32, 13-28, 30-33	189.29	1892.9	1.0375	1.0375

Case 2: This case explores impacts of DERs and SVCs on the optimal operation of distribution systems by adding SVCA, GA, and GB into the system. Rec-c and Rec-d are completed in 12 seconds and 61 seconds, respectively. All variable matrices corresponding to switched-on lines are rank one, and (18) is satisfied in both models. Thus, same as Case 1, a feasible and good-enough solution to (9) can be recovered.

Solutions of Rec-c and Rec-d as well as the two base cases BS-c and BS-d without network reconfiguration are compared in Table IV. It is noted that in Rec-c, phase a voltages of buses 7 and 18 reach their upper limits. Primary and secondary sides of the ideal transformer l(19,20) are reversed as compared to the original system topology, i.e., bus 19 is at the downstream of bus 20. That is, l(19,20) still works as a step-up transformer with the tap ratio of 1/0.9967.

Table IV also shows that the topology reconfiguration results of Rec-c and Rec-d are identical, but significantly differ from those in Case 1, which demonstrates the impacts of DERs and SVCs on the optimal network reconfiguration. In addition, in Case 2, after reconfiguration, the system contains two main radial laterals (buses 13, 27-30, 33 and buses 8, 17-26, 31-35), with 6 and 15 buses respectively, which supply very different amounts of loads (i.e., 6760kW and 8190kW). Furthermore, after network reconfiguration, the two DERs are connected towards the ends of the two radial laterals for holding up terminal bus voltages and reducing line currents, so as to reduce system losses. In turn, Rec-c and Rec-d reduce system losses by 50.76% and 50.97%, as compared to BS-c and BS-d.

Dispatches of DERs and SVCs in Rec-d are detailed in Table V. Results show that active power output of GB reaches the upper limit because of its relatively low operation cost. Apparent power through the three-phase inverter of GB also reaches its upper limit, which shows GB has also fully contributed its reactive power capacity. Reactive power outputs of SVCA in phase *a* and GA in three phases all reach their upper limits. That is, reactive power capacities of both SVCA and DERs are fully utilized to elevate voltage profiles and minimize system losses, so as to reduce the total system operation cost.

TABLE IV RESULTS IN CASE 2

	Switched-Off Line	Objective	Losses	Tap Rat	io (p.u.)
	Switched-Off Line	(\$)	(kW)	(6-7)	(19-20)
Rec-c	16-17,17-31,26-27,32-33	1740.97	377.51	1.0200	0.9967
Rec-d	16-17,17-31,26-27,32-33	1741.22	379.80	1.0125	0.9875
BS-c	17-31, 8-32, 13-28, 30-33	1780.51	766.65	1.0233	1.0182
BS-d	17-31, 8-32, 13-28, 30-33	1781.44	774.56	1.0125	1.0250

	TABLE V DERS AND SVCs DISPATCHES IN REC-D OF CASE 2							
DI	Substation Bus		GA		GB		SVCA	
Phase	$P_g(kW)$	$Q_g(kvar)$	$P_g(kW)$	$Q_g(kvar)$	$P_g(kW)$	$Q_g(kvar)$	$Q_g(kvar)$	
а	4239.1	1607.5	1160.5	720	1250	630.5	850	
b	4247.4	2400.0	1027.3	780	1250	510.1	/	
c	4150.6	2587.9	1162.8	700	1250	510.1	/	

In Rec-d of Case 2, active power dispatches of renewable DERs all reach their upper limits. This is because feed-in tariff of renewable DER is smaller than electricity price of the main grid and operation cost of conventional DERs, and in turn utilities prefer to dispatch as much renewables as possible without violating system constraints. Indeed, as more renewable DERs would impact system voltage profiles, further adjusting VR tap ratios could help facilitate a deeper utilization of available active power energy from renewable DERs. The impact of VRs for accommodating more renewables DERs is further studied. We adopt the same network configuration result from Case 2, while enlarging P_q^{est} and S_q^{max} of renewable DER GB to 1800kW and 2000kVA respectively and rerunning the Rec-d model. Result is compared with Rec-d of Case 2 in Table VI. It can be seen that the objective value decreases because more renewable energy are accommodated. However, in order to mitigate the impact of increased renewable DER injection to voltage profiles, VR l(6,7) acts as a step-down transformer and VR l(19.20) works as a step-up transformer with a higher tap ratio of 1/0.9625, which together help raise the voltage profile of branch 19-17-18.

TABLE VI IMPACT OF VRS TO ACCEPTED RENEWABLES

	Objective (\$)_	Tap Ratio		P_g (kW)		
	σσ ιστι (ψ).	(6-7)	(19-20)	а	b	С
Case 2	1740.97	1.0125	0.9875	1250	1250	1250
Enlarged GB Case	1680.57	0.9625	0.9625	1800	1800	1800

Case 3: This case studies the impact of CILs on the network reconfiguration and system optimal operation. Two three-phase pure resistive CILs are added at buses 9 and 26, with 40kW capacity per phase at the nominal voltage. Rec-c and Rec-d are completed in 70 seconds and 184 seconds, respectively. All variable matrices corresponding to switched-on lines are rank one and condition (18) is also satisfied in both models for original problem (9)'s solution recovery. Solutions of the two models are compared in Table VII.

TABLE VII RESULTS IN CASE 3

	Switched-Off Line	Objective	Tap Ratio (p.u.)		
	Switched-Off Line	(\$)	(6-7)	(19-20)	
Rec-c	16-17,17-31,26-27,32-33	1766.62	0.9500	0.9500	
Rec-d	16-17,17-31,26-27,32-33	1766.62	0.9500	0.9500	

It is observed that Rec-c and Rec-d derive exactly the same solution. Network topology configuration results from these two models are also same as those in Case 2, while the most prominent difference exists in the tap ratio of transformer l(6,7). Considering a CIL's power consumption is proportional to the squared terminal voltage magnitude, a higher voltage magnitude will lead to a larger active power consumption and thus a higher operation cost. In Case 3, the system voltage profile is optimally regulated for the best tradeoff between reduced line losses and increased active power consumptions of CILs, since a higher voltage profile generally implies lower line losses but higher power consumptions of CILs and vice versa. Ideal transformer l(19,20) works as a step-up transformer with the tap ratio of 1/0.9500, while bus 20 is reconfigured as the upstream of bus

19. While VR l(6,7) acts as a step-down transformer, and its tap ratio reaches the lower bound for reducing CILs' power consumptions.

C. Impact of Maximum Meshed Sub-Network Strategy

Computational impact of applying the maximum meshed sub-network strategy is studied in this section. Rec-c models of modified IEEE 34-bus and IEEE 123-bus systems are recalculated without considering the maximum meshed subnetwork strategy. Results are shown in Table VIII. It is observed that numbers of binary variables and continuous variables W are both reduced after the maximum meshed subnetwork strategy is applied. Indeed, a smaller number of binary variables could reduce number of nodes being searched by the branch-and-bound algorism, and a smaller number of continuous variables would reduce computational time of each SDP node of an MISDP problem, which both provide direct time saving in solving MISDP models. Consequently, computational performance after applying the maximum meshed sub-network strategy has been improved to certain extend in various system studies.

TABLE VIII COMPARISON WITH AND WITHOUT CONSIDERING MAXIMUM MESHED SUB-NETWORK STRATEGY

			With Maximum	Without Maximum
			Meshed Sub-network	Meshed Sub-
			Strategy	network Strategy
	Computation	Case 1	31	74
IEEE	time	Case 2	12	28
34-	(second)	Case 3	70	77
bus	# of card(I)		63	93
-	# 0	of W	240	348
IEEE	Computation	time (second)	328	430
123-	# of <i>a</i>	ard(I)	144	207
bus	# 0	of W	564	816

D. The Modified 392-Bus System

A 392-bus system [27], which is modified based on an IEEE 8500-node system, is further studied to illustrate the computational performance of the proposed model on large-scale distribution systems. The IEEE 8500-node system is modified by combining adjacent short line segments, so that all lines in the resulting system are no shorter than 250 meters. The reason for such a system modification is that line admittances in the original IEEE 8500-node system differ in several orders of magnitude, which introduces significant numerical issues when solving the MISDP model. Besides combining ultra-short lines, rescaling voltage and power bases is also adopted to further resolve the numerical issue.

Two cases with three and four switchable tie-lines are studied and compared, as illustrated in Table IX. Threshold of the BAB relative gap is set as 0.05%. Specifically, when the number of switchable tie-lines increases from 3 to 4, more than 43.75% switchable distribution lines are included in meshed sub-networks, which significantly increases the number of nodes to be explored and the computational time. In turn, for large-scale systems with more switchable tie-lines, solving MISDP models to a small BAB relative gap in a reasonable time remains a challenging issue to be addressed.

	# of Tie- Lines	# of Maximum Meshed Sub- Networks	# of Switch- able Lines	Model	# of Nodes Explored	Objective (\$)	Time (s)
	2	1	32	Rec-c	314	1104.08	186
	3	1	32	Rec-d	1718	1104.26	1032
	4	2	46	Rec-c	2208	1101.24	1406
4	2	40	Rec-d	11326	1101.95	8734	

Indeed, two main factors would impact computational performance of the proposed MISDP-based unbalanced distribution system network reconfiguration approach: (i) the number of switchable lines, i.e., the number of binary variables, which may impact the efficiency of the BAB procedure, and (ii) the scale of distribution systems, which would impact the computational time of each SDP node in the BAB tree. The maximum meshed sub-network concept and the chordal relaxation approach proposed in this paper intend to handle these two challenges. It is observed that SDP models have been widely used in various areas, while the use of MISDP models is still very limited due to the lack of high performance commercial solvers. It is expected that with the development of effective algorithms specifically aiming at MISDP problems [30], the application of MISDP models for solving distribution system operation problems could become more flourish in the future. Furthermore, the following strategies are explored to further improve the computational performance of the proposed approach:

- Solve Rec-c and Rec-d sequentially: With extra binary variables to indicate tap positions, Rec-d model can accurately represent physical operation behaviors of VRs, at the cost of high computational burden. Indeed, Table IX shows that the computational time of Rec-d could be 9 times longer than that of Rec-c on a large system. On the other hand, case study results of several systems including modified IEEE 34-bus, modified IEEE 123-bus [27] and 392-bus systems show that these two models derive same or very similar network topology configuration results. Considering this fact, a sequential strategy can be adopted for large distribution systems. First solve Rec-c to obtain the optimal network topology configurations, and then solve Rec-d with fixed network topology configuration, namely fixing I in Rec-d with results from Rec-c to determine the final tap positions of VRs and optimal dispatches of DERs.
- Handle Degree-two bus with zero injections: Degree-two buses with zero power injections are those connected by two lines without any other system assets, which are commonly seen in distribution systems, such as buses 1, 10, and 15 in Fig. 3. If such a bus is contained in a maximum meshed subnetwork, bus 15 in Fig. 3 for instance, switching off either line 13-15 or 15-16 will have very similar impacts on final operation solutions, since the current flowing through the remaining switched ON line is close to 0. Thus, one of the two connected lines of a degree-two bus with zero power injections can be modeled as un-switchable, so Reduced-complexity semidefinite as to further reduce the number of binary variables.

This paper proposes an optimal network reconfiguration model for unbalanced distribution systems, while considering co-optimized operations of voltage regulation devices and different types of DERs with unbalanced three-phase AC power flow constraints. The network reconfiguration problem is formulated as an MISDP model for the first time, in which the distribution network topology structure is explored to reduce the problem dimension, and chordal relaxation is adopted to improve solution performance. Numerical results illustrate that network reconfiguration could significantly reduce distribution system operation cost, especially when coordinated with optimal dispatches of DERs and voltage regulation devices. Two VR models with continuous and discrete tap ratios are compared in terms of effectiveness and performances. Considering the computational burden with increased number of switchable lines and the practical scale of distribution systems, acceleration strategies are explored to enhance the computational performance of the proposed network reconfiguration approach for DSOs to optimally derive operation strategies of emerging distributions systems.

REFERENCES

- S. Civanlar, J.J. Grainger, H. Yin, and S.S.H. Lee, "Distribution feeder reconfiguration for loss reduction," *IEEE Trans. Power Del.*, vol. 3, no. 3, pp. 1217-1223, Jul. 1988.
- [2] F. Ding and K.A. Loparo, "Hierarchical decentralized network reconfiguration for smart distribution systems-part I: problem formulation and algorithm development," *IEEE Trans. Power Syst.*, vol. 30, no. 2, pp. 1458-1459, Mar. 2015.
- [3] Y. Ch, S.K. Goswami, and D. Chatterjee, "Effect of network reconfiguration on power quality of distribution system," *Electr. Power Energy Syst.*, vol. 54, pp. 664-71, 2014.
- [4] Y. Wu, C. Lee, L. Liu, and S. Tsai, "Study of reconfiguration for the distribution system with distributed generators," *IEEE Trans. Power Del.*, vol. 25, no. 3, pp. 1678-1685, Jul. 2010.
- [5] R.S. Rao, K. Ravindra, K. Satish, and S.V.L. Narasimham, "Power loss minimization in distribution system using network reconfiguration in the presence of distributed generation," *IEEE Trans. Power Syst.*, vol. 28, no. 1, pp. 317-325, Mar. 2013.
- [6] S. Chen, W. Hu, and Z. Chen, "Comprehensive cost minimization in distribution networks using segmented-time feeder reconfiguration and reactive power control of distributed generators," *IEEE Trans. Power* Syst., vol. 31, no. 2, pp. 983-993, Mar. 2016.
- [7] X. Bai, H. Wei, K. Fujisawa, and Y. Wang, "Semidefinite programming for optimal power flow problems," *Int. J. Elect. Power Energy Syst.*, vol. 30, no. 6-7, pp. 383-392, 2008.
- [8] E.D. Anese, H. Zhu, and G.B. Giannakis, "Distributed optimal power flow for smart microgrids," *IEEE Trans. Smart Grid*, vol. 4, no. 3, pp. 1464-1475, Sep. 2013.
- [9] J. Lavaei and S.H. Low, "Zero duality gap in optimal power flow problem," *IEEE Trans. Power Syst.*, vol. 27, no. 1, pp. 92-106, Feb. 2012.
- [10] R.A. Jabr, R. Singh, and B.C. Pal, "Minimum loss network reconfiguration using mixed-integer convex programming," *IEEE Trans. Power Syst.*, vol. 27, no. 2, pp. 1106-1115, May 2012.
- [11] J.A. Taylor and F.S. Hover, "Convex models of distribution system reconfiguration," *IEEE Trans. Power Syst.*, vol. 27, no. 3, pp. 1407-1413, Aug. 2012.
- [12] Q. Peng, Y. Tang, and S.H. Low, "Feeder reconfiguration in distribution networks based on convex relaxation of OPF," *IEEE Trans. Power Syst.*, vol. 30, no. 4, pp. 1793-1804, Jul. 2015.
- [13] Y. Liu, J. Li, and L. Wu, "Distribution system restructuring: distribution LMP via Unbalanced ACOPF," *IEEE Trans. Smart Grid, DOI:* 10.1109/TSG.2016.2647692, 2017.
- [14] F. Ding and K.A. Loparo, "Feeder reconfiguration for unbalanced

- distribution systems with distributed generation: a hierarchical decentralized approach," *IEEE Trans. Power Syst.*, vol. 31, no. 2, pp. 1633-1642, Mar. 2016.
- [15] A. Zidan, H.E. Farag, and E.F. El-Saadany, "Network reconfiguration in balanced and unbalanced distribution systems with high DG penetration," in Proc. IEEE PES General Meeting, Detroit, MI, USA, Jul. 2011.
- [16] A. Zidan and E.F. El-Saaddany, "Network reconfiguration in balanced and unbalanced distribution systems with variable load demand for loss reduction and service restoration," in Proc. IEEE Power and Energy Soc. General Meeting, San Diego, CA, USA, Jul. 2012.
- [17] E.D. Anese and G.B. Giannakis, "Sparsity-leveraging reconfiguration of smart distribution systems," *IEEE Trans. Power Del.*, vol. 5, no. 2, pp. 487-497, Apr. 2014.
- [18] M.R. Dorostkar-Ghamsari, M. Fotuhi-Firuzabad, M. Lehtonen, and A. Safdarian, "Value of distribution network reconfiguration in presence of renewable energy resources," *IEEE Trans. Power Syst.*, vol. 31, no. 3, pp. 1879-1887, May 2016.
- [19] B. Zhang, A.Y.S. Lam, A.D. Dominguez-Garcia, and D. Tse, "An optimal and distributed method for voltage regulation in power distribution systems," *IEEE Trans. Power Syst.*, vol. 30, no. 4, pp. 1714-1726, May 2015.
- [20] H.M. Khodr, J. Martínez-Crespo, M.A. Matos, and J. Pereira, "Distribution systems reconfiguration based on OPF using benders decomposition," *IEEE Trans. Power Del.*, vol. 24, no. 4, pp. 2166-2176, Jul. 2010.
- [21] S. Bose, S. Low, T. Teeraratkul, and B. Hassibi, "Equivalent relaxations of optimal power flow," *IEEE Trans. Autom. Control*, vol. 60, no. 3, pp. 729-742, Mar. 2015.
- [22] M.S. Andersen, A. Hansson, and L. Vandenberghe, "Reduced-complexity semidefinite relaxations of optimal power flow problems," IEEE Trans. Power Syst., vol. 29, no. 4, pp. 1855-1863, Jul. 2014.
- [23] Y. Liu, J. Li, L. Wu and T. Ortmeyer, "Chordal relaxation based ACOPF for unbalanced three-phase distribution system with DERs and voltage regulation transformers", *IEEE Trans. Power Syst.*, DOI: 10.1109/TPWRS.2017.2707564,2017.
- [24] M. O'boyle, "Who should own and operate distributed energy resources?" [Online]. Available: http://docplayer.net/14659309-Whoshould-own-and-operate-distributed-energy-resources.html. Accessed: Sep. 25, 2017.
- [25] E.D. Anese, S.V. Dhople, and G.B. Giannakis, "Photovoltaic inverter controllers seeking AC optimal power flow solutions," *IEEE Trans. Power Syst.*, vol. 31, no. 4, pp. 2809-2823, Jul. 2016.
- [26] B.A. Robbins, H. Zhu, and A.D. Dominguez-Gracia, "Optimal tap setting of voltage regulation transformers in unbalanced distribution systems," *IEEE Trans. Power Syst.*, vol. 31, no. 1, pp. 256-267, Jan. 2016
- $[27] \ http://www.clarkson.edu/{\sim}lwu/data/Reconfig/.$
- [28] https://yalmip.github.io/?n=Solvers.LMILAB.
- [29] https://www.mosek.com/.
- [30] T. Gally, M.E. Pfetsch, and S. Ulbrich, "A framework for solving mixed-integer semidefinite programs," *Technical report, Optimization-Online*, 2016.

BIOGRAPHIES

Yikui Liu (S'15) received the B.S. degree in electrical engineering and automation from Nanjing Institute of Technology, China, in 2012 and the M.S. degree in power system and automation from Sichuan University, China, in 2015. He is currently pursuing the Ph.D. degree with Electrical and Computer Engineering Department, Clarkson University, USA. His current research interests are power market and OPF in distribution system.

Jie Li (M'14) received the B.S. degree in information engineering from Xi'an Jiaotong University in 2003 and the M.S. degree in system engineering from Xi'an Jiaotong University, China in 2006, and the Ph.D. degree from the Illinois Institute of Technology (IIT), Chicago, in 2012. From 2006 to 2008, she was a Research Engineer with IBM China Research Lab. From 2012 to 2013, she was a Power System Application Engineer with GE Energy Consulting. Presently, she is an Assistant Professor in the Electrical and Computer Engineering Department at Clarkson University. Her research interests include power systems restructuring and bidding strategy.

Lei Wu (SM'13) received the B.S. degree in electrical engineering and the M.S. degree in systems engineering from Xi'an Jiaotong University, Xi'an, China, in 2001 and 2004, respectively, and the Ph.D. degree in electrical engineering from Illinois Institute of Technology (IIT), Chicago, IL, USA, in 2008. From 2008 to 2010, he was a Senior Research Associate with the Robert W. Galvin Center for Electricity Innovation, IIT. He worked as summer Visiting Faculty at NYISO in 2012. Currently, he is an Associate Professor with the Electrical and Computer Engineering Department, Clarkson University, Potsdam, NY, USA. His research interests include power systems operation and planning, energy economics, and community resilience microgrid.